Geotechnical Testing Journal, Vol. 33, No. 2
Paper ID GTJ102278
Available online at: www.astm.org

TECHNICAL NOTE

P. Anbazhagan[1] *and T. G. Sitharam*[2]

Relationship between Low Strain Shear Modulus and Standard Penetration Test *N* Values

ABSTRACT: A low strain shear modulus plays a fundamental role in the estimation of site response parameters. In this study an attempt has been made to develop the relationships between standard penetration test (SPT) *N* values with the low strain shear modulus (G_{max}). For this purpose, field experiments SPT and multichannel analysis of surface wave data from 38 locations in Bangalore, India, have been used, which were also used for seismic microzonation project. The in situ density of soil layer was evaluated using undisturbed soil samples from the boreholes. Shear wave velocity (V_s) profiles with depth were obtained for the same locations or close to the boreholes. The values for low strain shear modulus have been calculated using measured V_s and soil density. About 215 pairs of SPT *N* and G_{max} values are used for regression analysis. The differences between fitted regression relations using measured and corrected values were analyzed. It is found that an uncorrected value of *N* and modulus gives the best fit with a high regression coefficient when compared to corrected *N* and corrected modulus values. This study shows better correlation between measured values of *N* and G_{max} when compared to overburden stress corrected values of *N* and G_{max}.

KEYWORDS: shear modulus, SPT, MASW, correlation

Introduction

Site amplification of seismic energy due to local soil conditions causing damage to built environment was amply demonstrated by many earthquakes during the past century (Guerrero earthquake (1985) in Mexico City, Spitak earthquake (1988) in Leninakan, Loma Prieta earthquake (1989) in San Francisco Bay Area, Kobe earthquake (1995) in Japan, Kocaeli earthquake (1999) in Turkey, and Bhuj earthquake (2001) in India). The recent 2001 Bhuj earthquake in India is another example, with notable damage at a distance of 250 km from the epicenter (Sitharam et al. 2001; GovindaRaju et al. 2004). These failures resulted due to effects of local soil conditions on the ground motion. Many cases have shown the changes in amplitude, period, and frequency of rock motion due to soil condition. Local site conditions also modify the spectral content and duration of ground motions. The response of a soil deposit depends on the frequency of the base motion and the geometry and dynamic properties of the soil layer above the bedrock. The seismic microzonation requires the shear wave velocity and shear modulus as input to estimate site specific ground response parameters (Anbazhagan and Sitharam, 2008a and 2009b; Sitharam and Anbazhagan, 2008a; Anbazhagan et al. 2009). The site specific ground response study requires the soil parameters of thickness (h), density (ρ), and shear modulus (G_{max}) of each layer as an input. The soil type and thickness of each layer are generally obtained by drilling boreholes and logging the borehole information (borelog). The in situ densities of each layer are usually obtained from the undisturbed soil samples collected in boreholes. In most cases, the shear modulus (G_{max}) for site response analysis is evaluated using relationships based on the standard penetration test (SPT) *N* values. These relationships are region specific, which depends on the type and characteristics of the soil in the respective region. It is not always fair to use existing correlations to obtain shear modulus for ground response studies without considering local soil condition. Hence, in this paper an attempt has been made to develop a relationship between SPT *N* value and G_{max} considering SPT and multichannel analysis of surface wave (MASW) data from Bangalore, India, where residual soils are abundant.

MASW is a seismic refraction method, which is widely used for sub-surface characterization. MASW is increasingly being applied to earthquake geotechnical engineering problems of seismic microzonation and site response studies (Anbazhagan and Sitharam 2008b). MASW can also be used for the geotechnical characterization of near surface materials (Park et al. 1999; Xia et al. 1999; Miller et al. 1999; Kanlı et al. 2006; Anbazhagan and Sitharam 2008c). In particular, it is used in geotechnical engineering to measure the shear wave velocity and dynamic properties (Sitharam and Anbazhagan 2008b) and to identify the sub-surface material boundaries and spatial variations of rocks (Anbazhagan and Sitharam 2009a). MASW is also used in the railway engineering to identify the degree of fouling and type of fouling (Anbazhagan et al. 2010). In this paper the low strain shear modulus (G_{max}) is evaluated using measured shear wave velocity obtained from MASW system and in situ density from undisturbed soil samples obtained at the same depth in the corresponding boreholes. These values are used to generate a correlation between SPT measured and corrected "*N*'" values and G_{max}. The developed relationships are compared with a similar relationship available in the literature.

Manuscript received December 9, 2008; accepted for publication December 18, 2009; published online March 2010.

[1]Dept. of Civil Engineering, Indian Institute of Science, Bangalore 560012, India. (Corresponding author), e-mail: anbazhagan@civil.iisc.ernet.in

[2]Dept. of Civil Engineering, Indian Institute of Science, Bangalore 560012, India.

General Setting of the Study Area

The area of study is limited to the Bangalore Metropolitan Area (Bangalore Mahanagar Palike) of about 220 km^2. Bangalore is

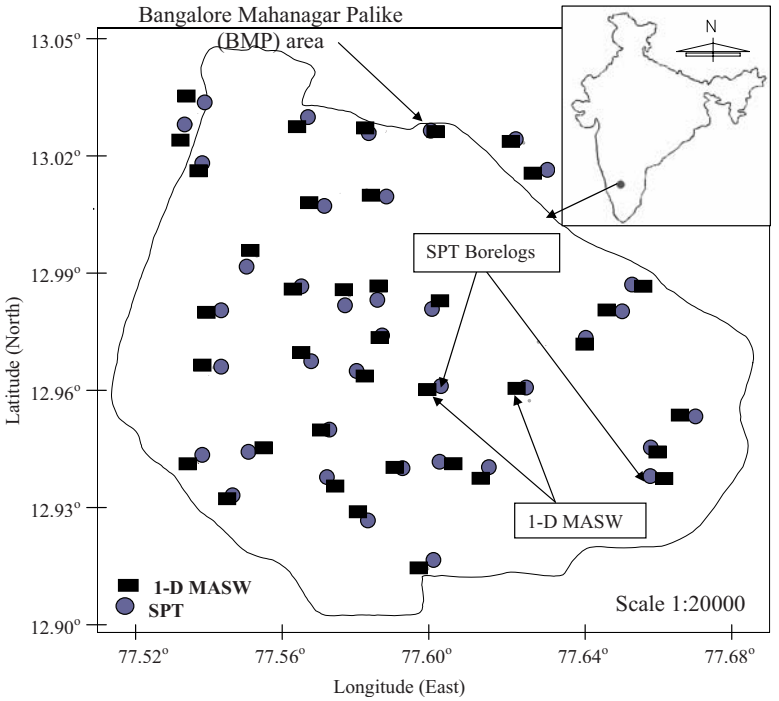

FIG. 1—*Testing locations of MASW survey with boreholes.*

situated on latitude 12°58′ North and longitude 77°36′ East and is at an average altitude of around 910 m above mean sea level. The basic geomorphology of the city comprises of a central Denudational Plateau and Pediment (towards the West) with flat valleys that are formed by the present drainage patterns. The central Denudational Plateau is almost void of any topology, and the erosion and transportation of sediments carried by the drainage network gives rise to the lateritic clayey alluvium seen throughout the central area of the city. The soil is mainly a product of strong weathering, ferruginous, clay mixture, and well drained. The main types of soil found here are red alluvium, sandy silts, alluvial clay, weathered rock (gravels), and soil fill material. The soil fill materials are a mixture of loose soil (excavated from constructions sites) and stones or building construction waste. Red alluvium (laterite) tropical residual soil is formed due to the erosion of the granitic and gneissic base rocks; this alluvium is ferruginous and is generally encountered in a clayey matrix. The erosion is caused by the natural drainage grid of lakes and streams throughout the city. Weathered rocks are generally granitic in composition; they are weathered from the parent rock and eventually combine with the sandy/clayey matrix.

Testing Programme

The field test locations for MASW were selected based on three criteria: (1) Sampling the range of soil types and conditions based on the SPT data, (2) flat surface free from noise, and (3) important places. The field MASW surveyed locations with SPT boreholes in Bangalore are shown in Fig. 1. The test locations were selected in such a way that these represent the entire city sub-surface information. In total, 38 one-dimensional (1D) MASW surveys have been carried out close to SPT borehole.

Multichannel Analysis of Surface Wave Testing

MASW is a geophysical method that generates a shear wave velocity (V_s) profile (i.e., V_s versus depth) by analyzing Raleigh-type surface waves recorded on a multichannel. A MASW system consisting of 24 channels Geode seismograph with 24 vertical geophones of 4.5 Hz capacity has been used in this investigation. The seismic waves are created by impulsive source of 15 lb (sledge hammer) with 300×300 mm^2 size hammer plate with number of shots. Figure 2 shows a typical MASW setup in the field with source and geophone arrangements. The source created waves are captured by receivers and further used for dispersion and inversion analysis. The optimum field parameters of source to first and last receiver, receiver spacing, and spread length of survey lines are selected in such a way that the required depth of information can be obtained. These field parameters are in conformity with the recommendations of Park et al. (2002).

Multichannel Analysis of Surface Wave Data Processing

The captured seismic waves through geophones are recorded for time duration of 1000 ms. The quality of the recorded data is verified in the field itself. Noisy records are rerecorded to get better signals of record. Typical recorded surface wave arrivals for a source to first receiver distance of 5 m and the processed data are shown in Fig. 3. Figure 3(*a*) and 3(*b*) shows the data before and after controlling noise during recording time, and Fig. 3(*c*) shows the noise reduced data (removing the noise during data processing). These recorded data are further used to get dispersion curves, which are used to extract shear wave velocity at the mid point of testing locations. Phase velocity can be calculated from the linear slope of each component on the swept-frequency record. The lowest analyzable frequency in this dispersion curve is around 4 Hz,

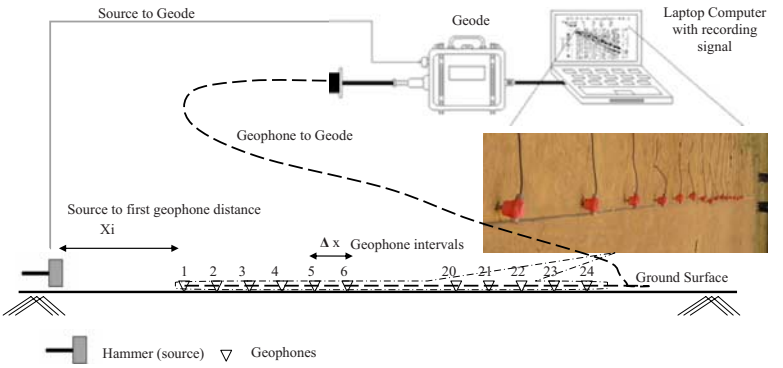

FIG. 2—*Typical field setup of source and receiver in MASW survey.*

and the highest frequency is 75 Hz. A typical dispersion curve along with signal amplitude and signal to noise ratio is shown in Fig. 4. Each dispersion curve is generated for corresponding signal to noise ratio of about 80 and above.

A shear wave velocity profile has been calculated using an iterative inversion process that requires the dispersion curve developed earlier as input. A least-squares approach allows automation of the process (Xia et al. 1999), which is inbuilt in SurfSeis. Typical 1D V_s profile obtained using MASW is shown in Fig. 5. The shear wave velocity values obtained from each survey line for the different layers fall within the recommendations of National Earthquake Hazards Reduction Program "V_s"-soil classification for different site categories IBC (2006) classification. Shear wave velocity obtained for the study area is used to estimate equivalent soil overburden V_s and is presented in Fig. 6. The average shear wave velocity for the depth "d" of soil is referred as V_H. The equivalent shear wave velocity up to a depth H (V_H) is computed as follows:

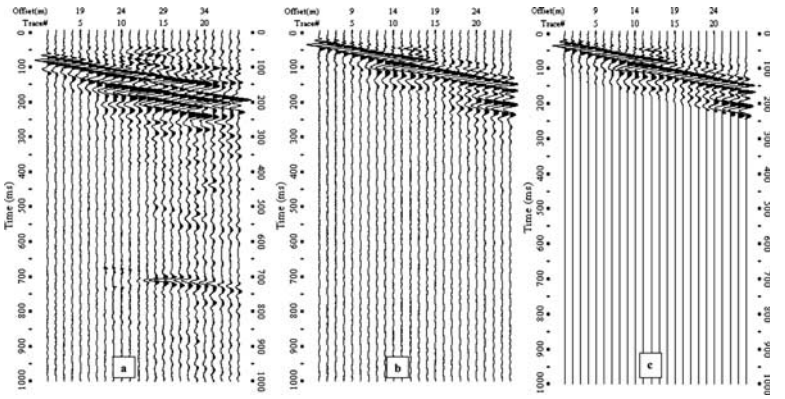

FIG. 3—*Typical seismic wave records: (a) Field record with more noise; (b) field record with reduced noise; and (c) processed data from (b).*

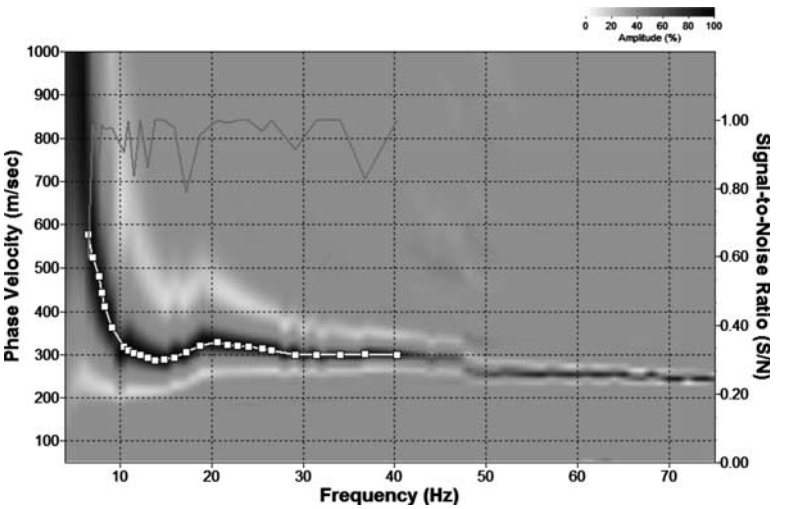

FIG. 4—*Typical dispersion curve obtained from MASW survey.*

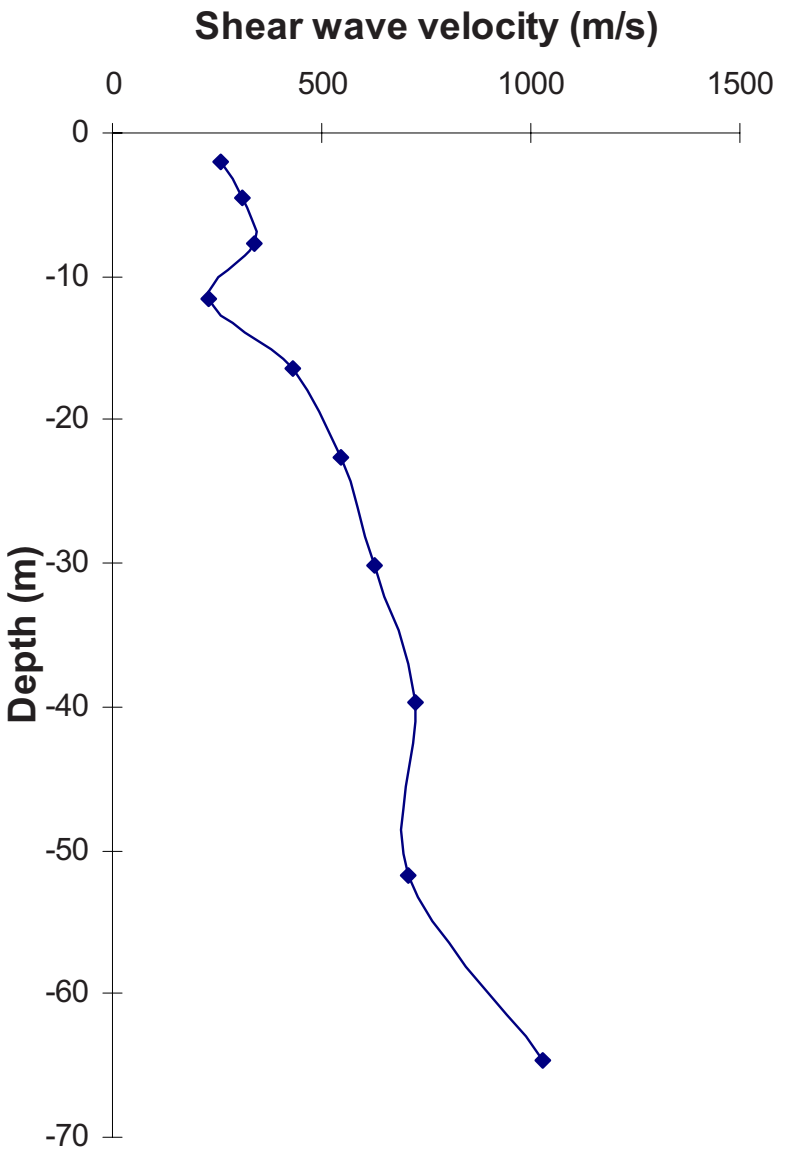

FIG. 5—*Typical shear wave velocity profiles obtained from MASW survey.*

$$V_H = \frac{\sum_{i=1}^{n} d_i}{\sum_{i=1}^{di} \left[\frac{d_i}{Vs_i} \right]} \quad (1)$$

where:

$H = \Sigma d_i$ = cumulative depth in m and

d_i and v_i denote the thickness (in m) and shear wave velocity (at a shear strain level of 10^{-5} or less, m/s) of the ith formation or layer respectively, in a total of n layers within the depth H.

The equivalent soil shear wave velocity varies from 100 to 450 m/s. Most of the area, having an average shear wave velocity of 200–300 m/s, can be classified as medium to dense soil.

Geotechnical Data

The SPT is one of the oldest, most, popular, and most common in situ tests used for soil exploration in soil mechanics and foundation engineering. This test is being used for many geotechnical projects because of the simplicity of the equipment and test procedure. In particular SPT tests are used for seismic site characterization, site response, and liquefaction studies towards seismic microzonation. This test is quite crude and depends on many factors due to the variations of applications carried out in the test and some equipment used in the test. The many factors includes the drilling methods, drill rods, borehole sizes and stabilization, sampler, blow count rate, hammer configuration, energy corrections, fine content, and test procedure (Schmertmann and Palacios 1979; Kovacs et al. 1981; Farrar et al. 1998; Sivrikaya and Toğrol 2006). The combined effect of all these factors can be accounted by applying the correction factors separately or together. The SPT N values may vary even for identical soil conditions because of sensitivity to operator techniques, equipment, malfunctions, and poor boring practice. So the SPT based correlations may be used for projects in preliminary stage or where there is a financial limitation, but for important projects, it is preferable to measure dynamic properties directly by using suitable field tests (Anbazhagan and Sitharam 2008c).

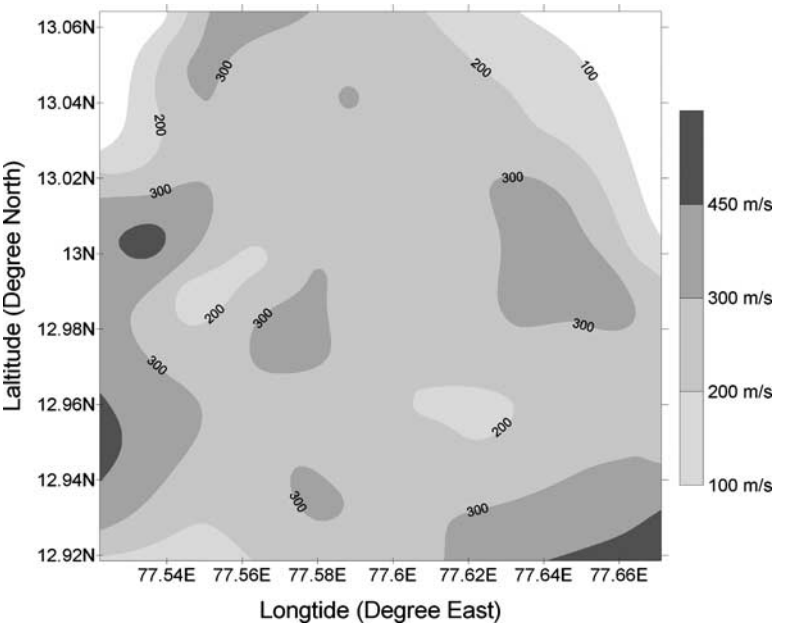

FIG. 6—*Soil overburden average shear wave velocity distribution in the study area.*

Boreholes used in this study have a diameter of 150 mm, drilled using hydraulic rotary drilling rigs up to the hard stratum. SPT tests were conducted at a regular sampling interval of 1.5 m in each borehole, and additional disturbed soil samples were also collected. Most of the penetration resistances (SPT *N* values) in the boreholes were measured using donut hammer. The undisturbed soil samples are collected according to Indian Standard IS 2132 (1986). The undisturbed soil sample is procured by driving the thin walled sampler of diameter of 100 and 450 mm length tube into the borehole at desired depth/change of strata. To avoid densification of soil samples due to hammering, the following precautionary steps are followed in the field: (1) The length of tube is marked on the driving rod and the driving is carried out carefully up to tube length (up to mark) by adjusting hammer height of fall, and (2) usually, the height of the hammer fall is limited to 20–40 cm. After ensuring complete penetration due to hammering, the tube is turned at least for two revolutions to shear the sample off at the bottom. The loose/disturbed soil in the upper end is removed and waxed on either end and taken to the laboratory. These samples are used to evaluate in situ densities of the soil layers. In most of the locations, the boreholes are drilled up to weathered rock and at few locations boreholes reached up to hard rock. A typical borehole with SPT *N* values with depth is shown in Fig. 7. These boreholes were also used for seismic microzonation of Bangalore and other studies (Sitharam et al. 2007; Sitharam and Anbazhagan 2008a). For the purpose of general identification of soil layers in the study area, a generalized classification of soil has been attempted using borehole information and is given in Table 1. Table 1 shows that the western part of the city/study area has lesser overburden thickness when compared to other areas and consist of medium to dense soil. The eastern part of the city has a thicker overburden, consisting of loose to dense soil with fill material.

N and V_S Corrections

The *N* values from field borelogs have been corrected for various corrections, such as (a) overburden pressure (C_N), (b) hammer energy (C_E), (c) borehole diameter (C_B), (d) presence or absence of liner (C_S), (e) rod length (C_R), and (f) fine content (C_{fine}) (Seed et al. 1983; 1985; Skempton, 1986; Youd et al. 2001; Cetin et al. 2004; Pearce and Baldwin 2005). Corrected *N* value. i.e., (N_{60}) is obtained using the following equation:

$$(N_1)_{60} = N \times (C_N \times C_E \times C_B \times C_S \times C_R) \tag{2}$$

The SPT *N* values recorded in the field increase with increasing effective overburden stress; hence overburden stress correction factor is applied (Seed and Idriss 1982). This factor is commonly calculated from the equation developed by Liao and Whitman (1986). However Kayen et al. (1992) has suggested the following equation, which limits the maximum C_N value to 1.7 and provides a better fit to the original curve specified by Seed and Idriss (1982):

$$C_N = 2.2/(1.2 + \sigma'_{vo}/P_a) \tag{3}$$

where:

σ'_{vo} = effective overburden pressure,
P_a = 100 kPa, and
C_N should not exceed a value of 1.7.

This empirical overburden correction factor is also recommended by Youd et al. (2001).

Another important factor that affects the SPT *N* value is the energy transferred from the falling hammer to the SPT sampler. The energy ratio (ER) delivered to the sampler depends on the type of hammer, anvil, lifting mechanism, and the method of hammer release. Where energy measurements cannot be made, careful observation and notation of the equipment and procedures are necessary to estimate the C_E value. The use of good-quality testing equipment and carefully controlled testing procedures will generally yield more consistent ERs. For liquefaction calculation, Yilmaz and Bagci (2006) took the C_E value as 0.7 for the SPT hammer donut type, delivering 60 % energy. In this study the delivered hammer energy is not measured, but the hammer used is similar to Yilmaz and Bagci (2006), so C_E is taken as 0.7.

The other correction for borehole diameter, rod length, and sampling methods are modified from Skempton (1986). The correction

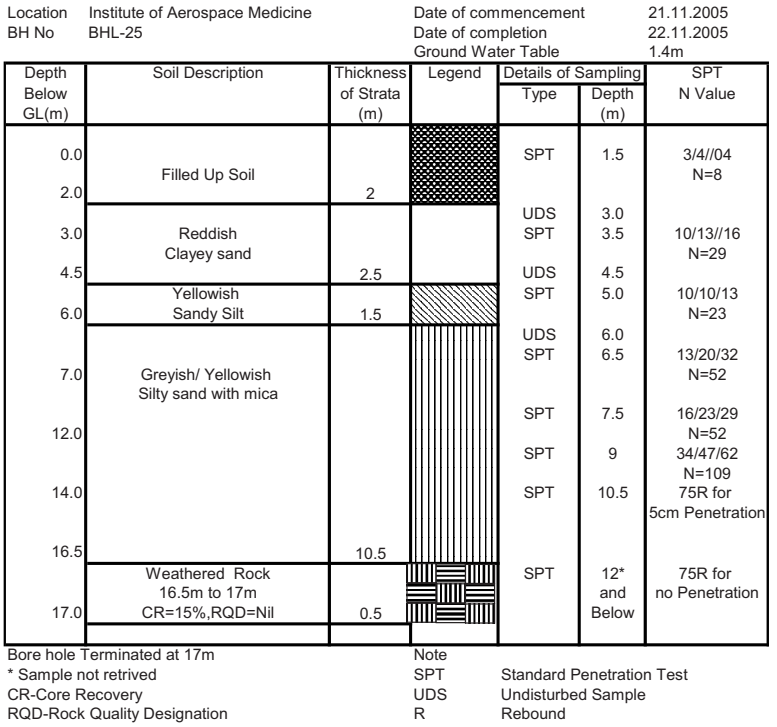

FIG. 7—*Typical borelog with the SPT N values.*

TABLE 1—*Soil distribution in Bangalore.*

	Soil Description with Depth and Direction			
Layer	Northwest	Southwest	Northeast	Southeast
First layer	Silty sand with clay, 0–3 m	Silty sand with gravel, 0–1.7 m	Clayey sand, 0–1.5 m	Soil fill material, 0–1.5 m
Second layer	Medium to dense silty sand, 3–6 m	Clayey sand, 1.7–8.5 m	Clayey sand with gravel, 1.5–4 m	Silty clay, 1.5–4.5 m
Third layer	Weathered rock, 6–11 m	Weathered rock, 8.5–18.5 m	Silty sand with gravel, 4–18.5 m	Sandy clay, 4.5–17.5 m
Fourth layer	Hard rock, below the 11 m	Hard rock, below 18.5 m	Weathered rock, 18.5–33.5 m	Weathered rock, 17.5–38.5 m
Fifth layer	Hard rock	Hard rock	Hard rock, below 33.5 m	Hard rock, below 38.5 m

TABLE 2—*Typical N correction table for borelog.*

Borehole										Water Table = 1.4 m / 19-11-2005			
						Correction Factors for							
Depth (m)	Field *N* Value	Density (kN/m^3)	TS (kN/m^2)	ES (kN/m^2)	C_N	Hammer Effect	Bore Hole Diameter	Rod Length	Sample Method	$(N_1)_{60}$	FC (%)	$\Delta(N_1)_{60}$	Corrected *N* Value, $(N_1)_{60cs}$
1.50	19	20.00	30.00	30.00	1.47	0.7	1.05	0.75	1	15.36	48	5.613	21
3.50	28	20.00	70.00	50.38	1.29	0.7	1.05	0.8	1	21.26	43	5.597	27
4.50	26	20.00	90.00	60.57	1.22	0.7	1.05	0.85	1	19.79	60	5.602	25
6.00	41	20.00	120.00	75.86	1.12	0.7	1.05	0.85	1	28.77	48	5.613	34
7.50	55	20.00	150.00	91.14	1.04	0.7	1.05	0.95	1	40.02	37	5.541	46
9.00	100	20.00	180.00	106.43	0.97	0.7	1.05	0.95	1	67.84	28	5.270	73
10.50	100	20.00	210.00	121.71	0.91	0.7	1.05	1	1	66.90	28	5.270	72
12.50	100	20.00	250.00	142.09	0.84	0.7	1.05	1	1	61.70	28	5.270	67

Note: TS: Total stress; ES: Effective stress; C_N: Correction for overburden correction; $(N_1)_{60}$: Corrected *N* value before correction for fine content; FC: Fine content; $\Delta(N_1)_{60}$: Correction for fine content; and $(N_1)_{60cs}$: Corrected *N* value.

factors are listed by Robertson and Wride (1998). The borehole diameter correction factor of 1.05 for 150 mm borehole diameter is used. The rod length correction factor (C_R) is applied based on the length of the rod. Sampler correction factor (C_S) for the presence or absence of liner is taken as 1.0 for standard sampler. The corrected N value $(N_1)_{60}$ is further corrected for fine content based on the revised boundary curves derived by Idriss and Boulanger (2004) for cohesionless soils as described below

$$(N_1)_{60cs} = (N_1)_{60} + \Delta(N_1)_{60} \tag{4}$$

$$\Delta(N_1)_{60} = \exp\left[1.63 + \frac{9.7}{FC + 0.001} - \left(\frac{15.7}{FC + 0.001}\right)^2\right] \tag{5}$$

where:

FC = percent fine content (percent dry weight finer than 0.075 mm).

Typical corrected N values for a borehole is shown in Table 2. Similarly SPT N corrected values with depth have been determined for all the boreholes.

Shear wave velocities are corrected for overburden stress using traditionally followed equation (Sykora 1987; Robertson et al. 1992; Andrus and Stokoe 2000; Youd et al. 2001; Juang et al. 2002; Andrus et al. 2004)

$$V_{s1} = V_s C_v \tag{6}$$

$$C_v = (P/\sigma'_{vo})^{0.25} \tag{7}$$

where:

V_{s1} = overburden stress corrected shear wave velocity and

C_v = factor to correct measured shear wave velocity for overburden pressure.

A maximum C_v value of 1.4 is generally applied to V_s at shallow depth (Andrus and Stokoe 2000). The overburden stress corrected shear wave velocity (V_{s1}) is evaluated for each layer, which is used to estimate the overburden stress corrected shear modulus $G_{\max 1}$.

TABLE 3—*Typical G_{max} calculation table.*

Depth (m)	V_s (m/s)	Density (g/cm^3)	Shear Modulus (MN/m^2)
0–1.2	252	1.90	121
1.2–2.7	158	1.90	47
2.7–4.6	149	1.90	42
4.6–7.0	283	1.90	152
7.0–10	343	1.90	224
10.0–13.7	328	1.90	204
13.7–18.4	386	2.00	298
18.4–24.2	508	2.00	516
24.2–31.4	582	2.20	745
31.4–39.3	804	2.20	1422

Relation between G_{max} and Standard Penetration Test N Values

The shear modulus at low strain level for soil layers has been determined using shear wave velocity from MASW and density from undistributed soil samples using Eq 8

$$G = \rho V_s^2 = \frac{\gamma}{g} V_s^2 \tag{8}$$

where:

ρ = density measured from the undisturbed sample and

V_s = shear wave velocity measured using the MASW testing.

G_{max} has been evaluated for corresponding depth of N values in the respective locations. Typical G_{max} calculations for one location are given in Table 3.

The correlation between measured G_{max} (calculated from measured shear wave velocity and density of each layer) to the measured SPT N values is attempted. From the 38 sets of MASW and SPT testing points, about 215 pairs of N and G_{max} values have been used for the regression analysis.

To obtain the practical relationship between shear modulus and N values and to understand data matching, different combinations of corrected and uncorrected values were attempted, as discussed below.

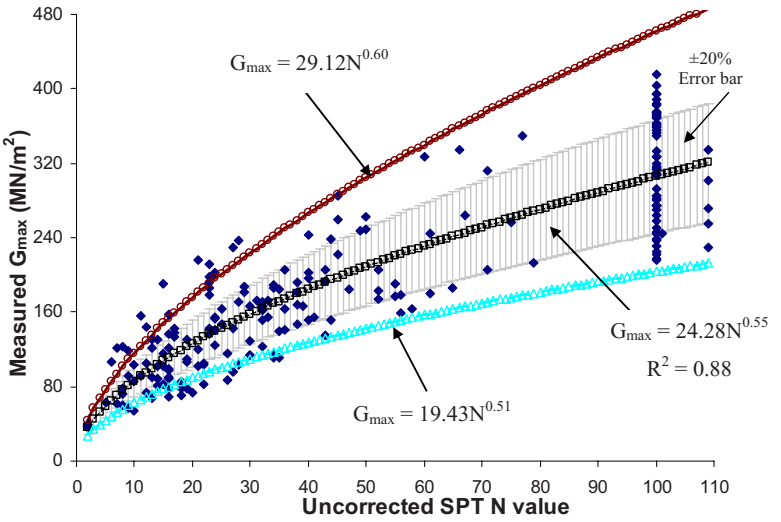

FIG. 8—*Shear modulus versus measured/uncorrected SPT N values.*

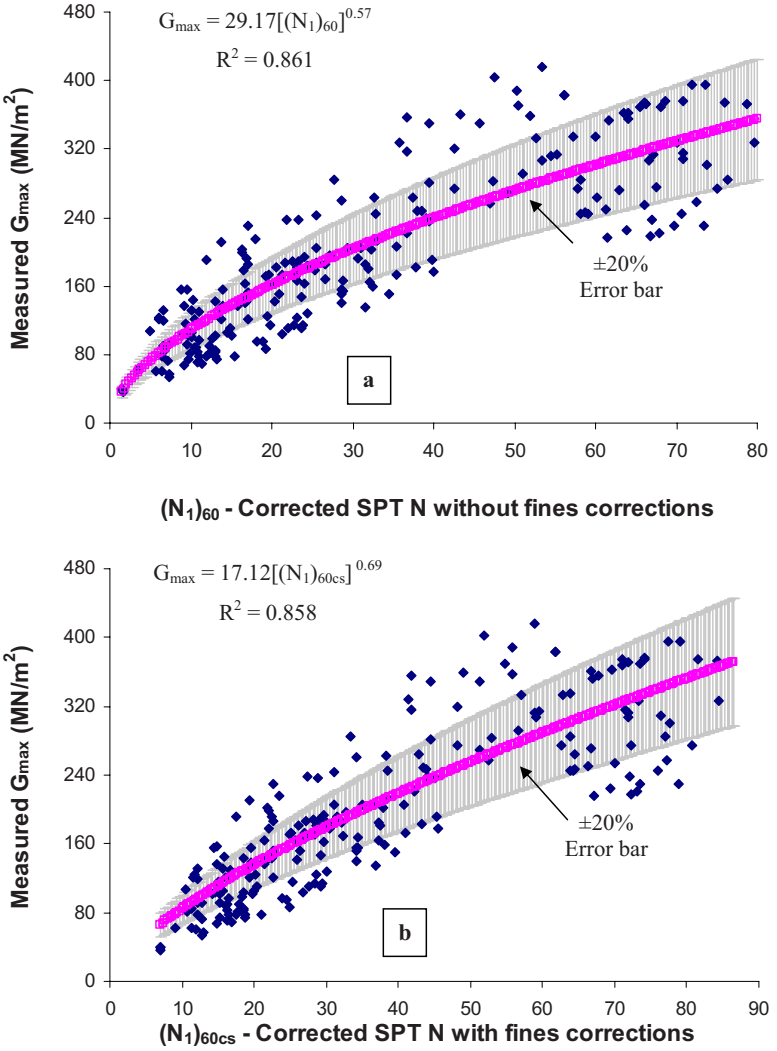

FIG. 9—*Shear modulus versus corrected SPT N values.*

Relation between Uncorrected Values

Correlation between measured values of SPT N and shear modulus (G_{max}) is presented in Fig. 8. The regression equation between G_{max} and N is given below

$$G_{max} = 24.28N^{0.55} \quad (9)$$

where:

G_{max} = low strain measured shear modulus in MN/m^2 and
N = measured SPT N value.

Figure 8 also shows the actual data and fitted equation with ±20 % error bars. The best fit equation has the regression coefficient R squared value of 0.88. In addition regression equations with 95 % confidence interval are shown in Fig. 8. The 95 % confidence bands enclose the area that one can be 95 % sure of the true curve. It gives a visual sense of how well the data defines the best fit curve (Motulsky 2008). Regression equations corresponding to 95 % confidence intervals are given in Eqs 10 and 11, respectively

$$G_{max} = 29.12N^{0.60} \quad \text{upper side of 95 \% confidence interval} \quad (10)$$

$$G_{max} = 19.43N^{0.51} \quad \text{lower side of 95 \% confidence interval} \quad (11)$$

Relation between Corrected N and Uncorrected G_{max} Values

To study the difference between corrected and uncorrected SPT N values in the regression equation, many combinations of plots were generated. Figure 9 shows the correlation between (a) corrected N values and measured modulus and (b) corrected N values with fine content correction and measured shear modulus. In the first case corrected N values are estimated excluding fine content correction factor according to Eq 2, and in the second case corrected N values are estimated including fine content correction factor according to Eq 4. The first one gives slightly higher R^2 value (0.86) when compared to the second one (R^2=0.858). The data range in the first case $[(N_1)_{60}]$ is distributed from 2 to about 90, but in the second case, it $[(N_1)_{60cs}]$ is distributed from 7 to about 90. For the purpose of developing the regression equation, any one of the corrected N value without or with fine content correction ($[(N_1)_{60}]$ or $[(N_1)_{60cs}]$) may be used. This is so because the corrected N values without or with

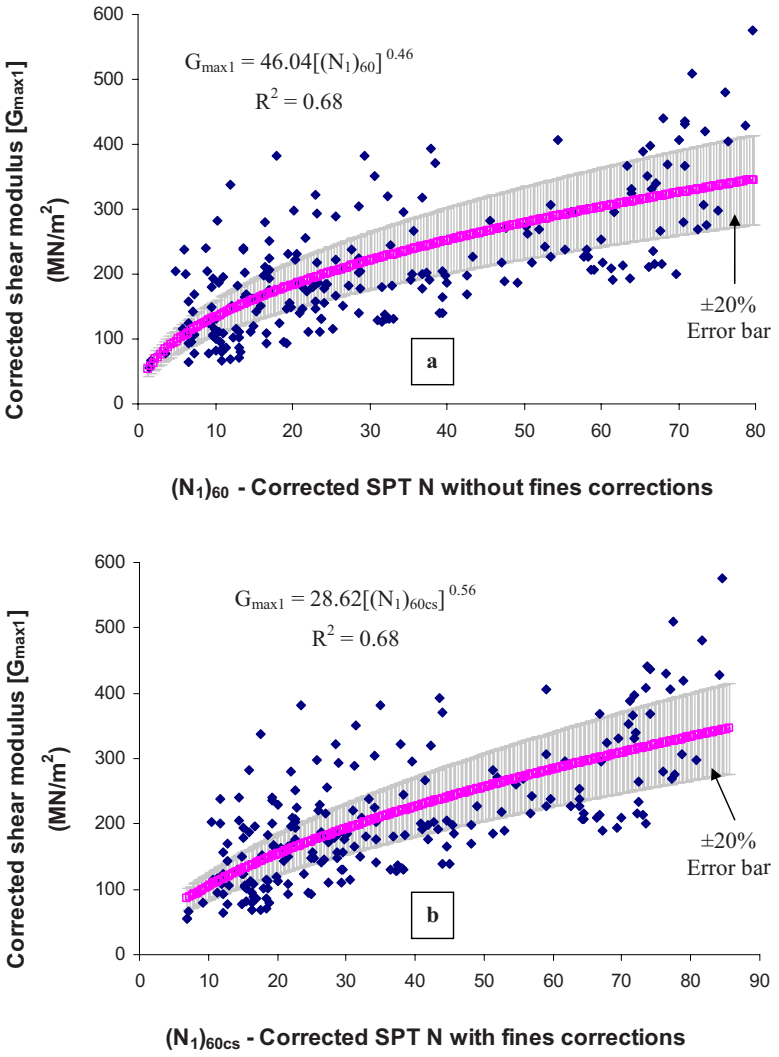

FIG. 10—*Corrected shear modulus ($G_{max\ 1}$) versus corrected SPT N values.*

fine content correction yield similar best fit equations and R^2 values. The developed regression equations for the corrected N values without or with considering fine content correction are given below: Without fine content correction

$$G_{max} = 29.17[(N_1)_{60}]^{0.57} \quad (12)$$

with fine content correction

$$G_{max} = 17.12[(N_1)_{60cs}]^{0.69} \quad (13)$$

Relation between Corrected N and Corrected G_{max} Values

The overburden stress corrected shear modulus has been evaluated using traditional applied V_s correction factor given in Eq 7. Figure 10(*a*) and 10(*b*) shows the corrected shear modulus ($G_{max\ 1}$) versus corrected N values of $(N_1)_{60}$ and $(N_1)_{60cs}$. It was found that the regression fit is poor and gives lower R^2 values when compared to corrected N and uncorrected G_{max} values. Also similar to the above results, the corrected N values without or with fine content correction gives similar fitted equation and R^2 values. The regression equation for the corrected shear modulus ($G_{max\ 1}$) and corrected N values without or with considering fine content correction is given below: Without fine content correction

$$G_{max\ 1} = 46.041[(N_1)_{60}]^{0.46} \quad (14)$$

with fine content correction

$$G_{max\ 1} = 28.62[(N_1)_{60cs}]^{0.56} \quad (15)$$

To trace out the problems, an attempt is made to use similar overburden stress correction factor applied to N values. The overburden stress corrected shear modulus of each layer has been evaluated using the correction factor given in Eq 3. Figure 11(*a*) and 11(*b*) shows the corrected shear modulus ($G_{max\ 2}$) versus corrected N values of $(N_1)_{60}$ and $(N_1)_{60cs}$. The regression fit is very poor and gives lower R^2 values when compared to corrected N and corrected $G_{max\ 1}$ values. The regression equation for the corrected shear modulus ($G_{max\ 2}$) and corrected N values without or with fine content correction is given below: Without fine content correction

$$G_{max\ 2} = 61.07[(N_1)_{60}]^{0.37} \quad (16)$$

With fine content correction

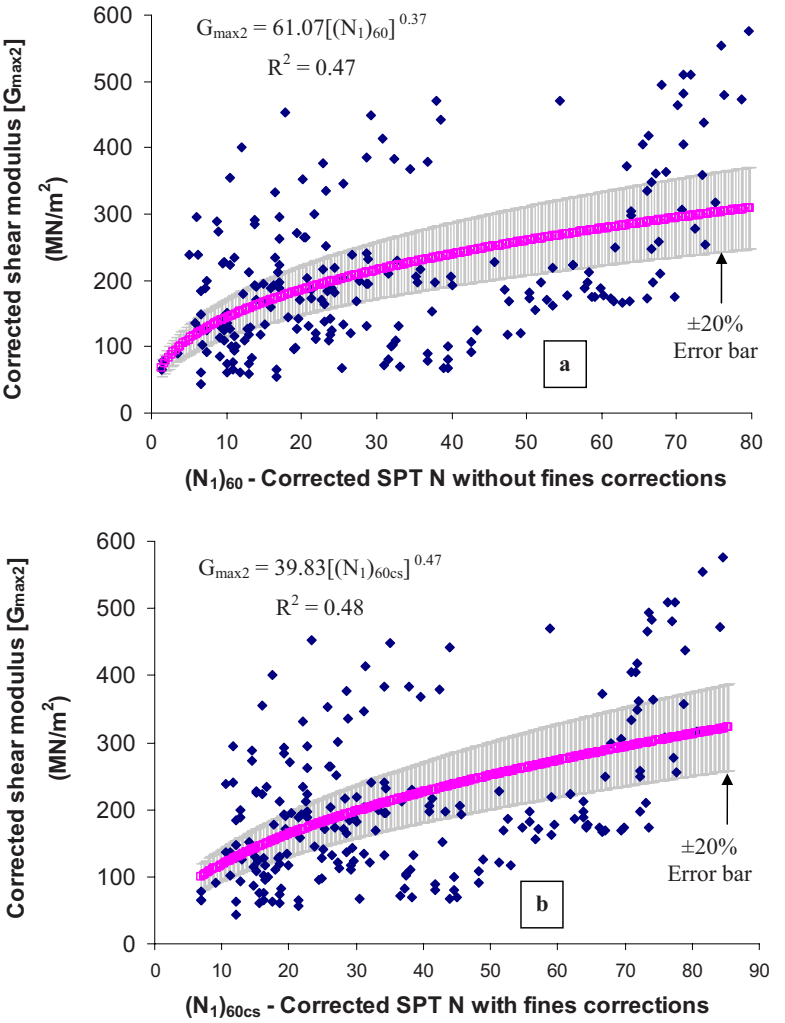

FIG. 11—*Corrected shear modulus ($G_{max\ 2}$) versus corrected SPT N values.*

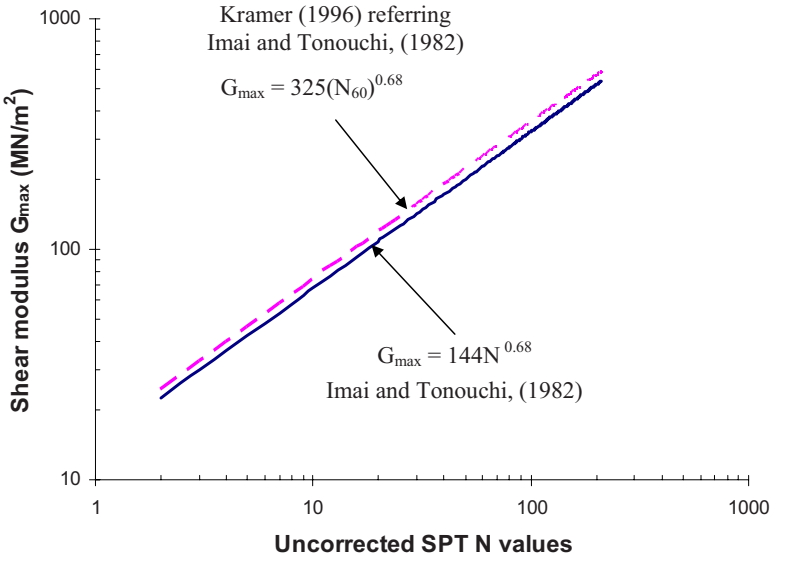

FIG. 12—*Comparison of shear modulus equations.*

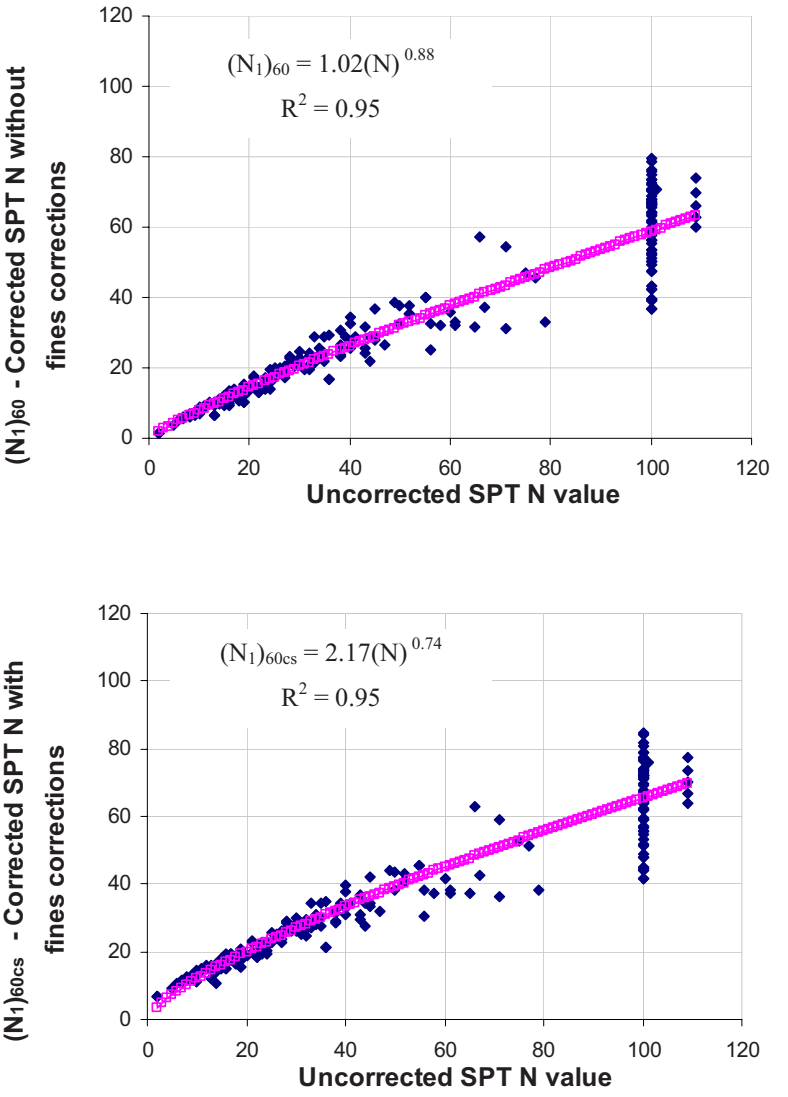

FIG. 13—*Corrected N without and with fine content correction versus observed N values.*

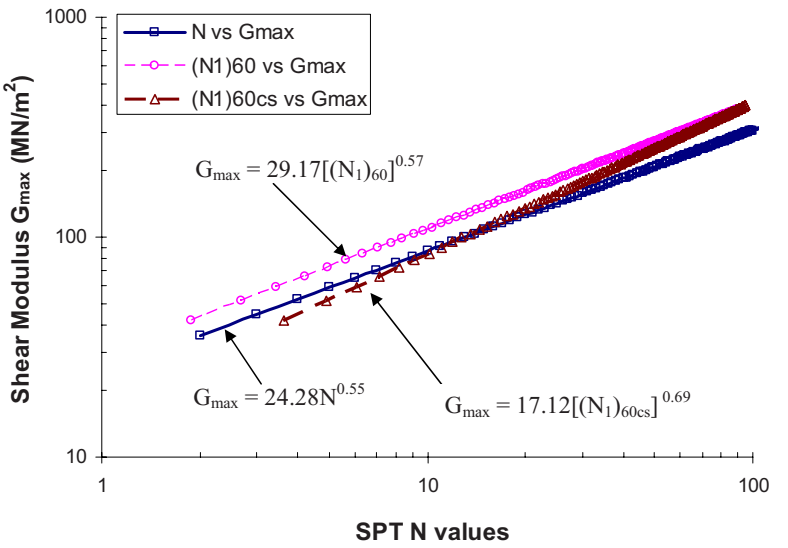

FIG. 14—*Comparison of shear modulus versus N values developed in this study.*

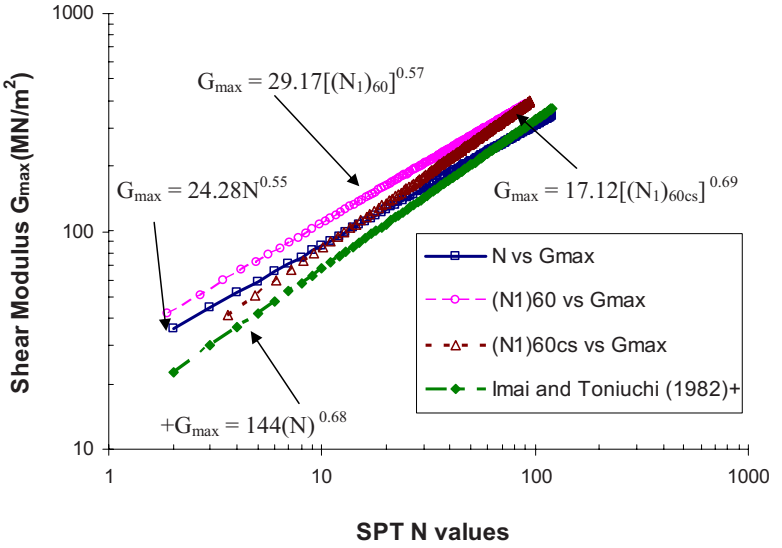

FIG. 15—*Comparison of relations developed in this study with Imai and Tonouchi (1982).*

$$G_{\max\ 2} = 39.83[(N_1)_{60cs}]^{0.47} \quad (17)$$

From this study, it is clear that the correlation between the normalized shear modulus and N does not give a better regression equation even though the data are same. It is necessary to review the traditionally used overburden stress correction factor for V_s. The traditional shear wave velocity correction factors may be revised in future based on these data or by including more data if available.

Results and Discussions

To validate N versus $G_{\max}$ relation presented in this study, it has been compared with existing relations available in the literature. Many regression equations between N, $(N_1)_{60}$, and $(N_1)_{60cs}$ with V_s and V_{s1} are available in the literature for different soils by different researchers, but limited regression equations are available for N versus $G_{\max}$. Popularly used correlations are given by Ohta and Goto (1978) [subsequent revision of data are presented by Seed et al. (1986)] and Imai and Tonouchi (1982). Seed et al. (1986) developed regression V_s relation by considering N_{60} (N values measured in SPT test delivering 60 % of theoretical free fall energy to the drill rods) and depth of soil in feet (D). Then by assuming unit weight (γ) of 1.92 g/cm^3 (120 pound per cubit foot), the $G_{\max}$ was calculated according to Eq 8, and $G_{\max}$ relation was developed. So comparing present equation with the Seed et al.. (1986) relation may not be appropriate. Hence, a comparison has been made with the study similar to the present study by Imai and Tonouchi (1982). Imai and Tonouchi (1982) developed N versus $G_{\max}$ relation using the average N values from single velocity layers, and also, N values of above 50 and below 1 are substituted for the number of blows required to achieve a penetration depth of 30 cm from actual amount of penetration achieved at 50 blows. Imai and Tonouchi (1982) used a large number of data from different age and soil types and presented the N values and shear modulus relation separately according to geology and soil type and together based on the overall data. The original equation proposed by Imai and Tonouchi (1982) is

$$G_{\max}(kg/cm^2) = 144N^{0.68} \quad (18)$$

The same equation was reproduced in Kramer (1996) for the corrected N values for sand, which is as follows (Kramer (1996) referring Imai and Tonouchi (1982)):

$$G_{\max}(kips/ft^2) = 325[N_{60}]^{0.68} \quad (19)$$

Figure 12 shows both the Eqs 18 and 19 using uncorrected values of N. In order to compare equations developed in our study, it is assumed that Eq 19 based corrected N values (N_{60}) as highlighted in the work of Kramer (1996). To compare the regression equations in a single plot, a relation between corrected N values [$(N_1)_{60}$ or $(N_1)_{60cs}$] to measured N values was developed, which is shown in Fig. 13. The best fit regression equation for the corrected N values without and with considering fine content correction [$(N_1)_{60}$ or $(N_1)_{60cs}$] and observed N values are given below

$$(N_1)_{60} = 1.02(N)^{0.88} \quad (20)$$

$$(N_1)_{60cs} = 2.17(N)^{0.74} \quad (21)$$

Figure 14 shows a comparison of the Eqs 9, 12, and 13 using the above Eqs 20 and 21. In Fig. 14, horizontal line gives uncorrected or corrected SPT N values based on the equation. If SPT N value of X is uncorrected for Eq 9, the same X is corrected N value without fine content correction for Eq 12 and corrected N value with fine content correction for Eq 13. This similar explanation also applies for Figs. 15 and 16. From Figs. 12 and 14, it is clear that corrected N values without fine content corrections yield a higher shear modulus ($G_{\max}$) against measured N values. The trends of the results for N values without considering fine content correction is similar to the one presented in Fig. 12. From Fig. 14, $G_{\max}$ equations developed using corrected N considering fine content correction (Eq 13) matches with $G_{\max}$ equation using measured N values (Eq 9) up to the N values of 20 and $G_{\max}$ equation using corrected N without considering fine content correction (Eq 12) for N values above 30. For the N values between 20 and 30, Eq 13 lies in between Eqs 9 and 12.

Figure 15 shows the comparison of equations developed in this study with Eq 18 presented by Imai and Tonouchi (1982). From Fig. 15, the developed relation between measured N values and

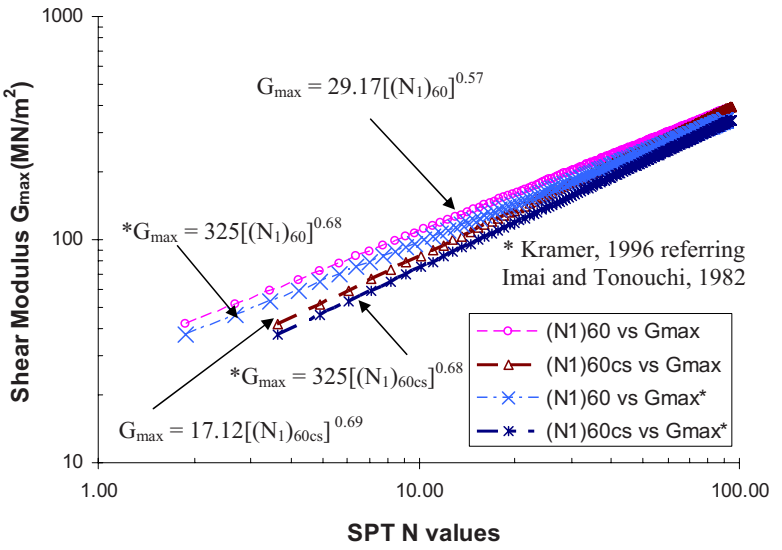

FIG. 16—*Comparison of relations developed in this study based on corrected N values with Kramer (1996) referring Imai and Tonouchi (1982).*

measured shear modulus matches well with the Eq 18 beyond the N value of 10; this may be attributed to soil type and number of data. In Imai and Tonouchi (1982) most of the data are below the N value of 10 (for clay and sand). However, in this study, soil is a mixture of sandy silt with clay and does not have many data for $N < 10$. Equation 13 shows a trend similar to that of Imai and Tonouchi (1982) equations. Figure 16 shows a comparison of equations developed in this study for corrected values, with Eq 19 presented by Kramer (1996). Shear modulus values have been evaluated considering $(N_1)_{60}$ and $(N_1)_{60cs}$ using Eq 19. From Fig. 15, regression relations developed in this study between corrected N values [$(N_1)_{60}$ and $(N_1)_{60cs}$] and measured shear modulus (Eqs 11 and 12) have similar trends. So in the equation given in Kramer (1996), the corrected N values might have been used. Developed equation based on the corrected N values match well with those of Kramer (1996). The correlations developed in this study used the measured SPT N values of up to 100 (refusal), whereas Imai and Tonouchi (1982) had used a measured N value of up to 50. Also, the proposed correlation is unique, independent of the lithology, soil grading, age, cementation, etc. The developed equations in this study can be directly used for soil type "silty sand or sandy silt with less clay content;" however for the important structures, the best way is to measure G_{max} directly using in situ seismic tests.

Conclusions

Regression relation between SPT N and G_{max} values have been developed using 215 pairs of SPT N and G_{max} from geotechnical borelogs and geophysical MASW data. The regression equation using measured values gives best fit and R^2 values when compared to the corrected N and corrected G_{max}. The regression relation between corrected N values without considering fine content correction [$(N_1)_{60}$] or with considering fine content correction [$(N_1)_{60cs}$] and G_{max} are also giving similar R^2 values. In the relation between corrected N values and measured shear modulus, any one of the corrected N values (without or with considering fine content correction) can be used for regression analysis. The relation between corrected N and G_{max} shows poor regression relation for the same data. The traditional overburden stress correction factors applied for shear wave velocity need a relook. The traditional shear wave velocity correction factors may be revised in the future based on these data or including more data if available. The proposed relations are comparable with the existing relations similar to this study. Existing relations were developed with many assumptions during the developing stage of geotechnical earthquake engineering (GEE). These relations have to be reviewed with present knowledge of GEE and may be updated and reproduced in the future. The developed equation between N and G_{max} is more suitable for residual soils (i.e., silty sand or sandy silt) with less percentage of clay content.

References

Anbazhagan, P., Indraratna, B., Rujikiatkamjorn, C., and Su, L., 2010, "Using a Seismic Survey to Measure the Shear Modulus of Clean and Fouled Ballast," *Geomech. Geoeng.*, Manuscript ID TGEO-2009-0027 (in press).

Anbazhagan, P. and Sitharam, T. G., 2008a, "Seismic Microzonation of Bangalore," *Journal of Earth System Science*, Vol. 117, No. S2, pp. 833–852.

Anbazhagan, P. and Sitharam, T. G., 2008b, "Site Characterization and Site Response Studies Using Shear Wave Velocity," *Journal of Seismology and Earthquake Engineering*, Vol. 10, No. 2, pp. 53–67.

Anbazhagan, P. and Sitharam, T. G., 2008c, "Mapping of Average Shear Wave Velocity for Bangalore Region: A Case Study," *J. Environ. Eng. Geophys.*, Vol. 13, No. 2, pp. 69–84.

Anbazhagan, P. and Sitharam, T. G., 2009a, "Spatial Variability of the Weathered and Engineering Bed Rock Using Multichannel Analysis of Surface Wave Survey," *Pure Appl. Geophys.*, Vol. 166, pp. 409–428.

Anbazhagan, P. and Sitharam, T. G., 2009b, "Estimation of Ground Response Parameters and Comparison with Field Measurements," *Indian Geotechnical Journal*, Vol. 39, No. 3, pp. 245–270.

Anbazhagan, P., Sitharam, T. G., and Vipin, K. S., 2009, "Site Classification and Estimation of Surface Level Seismic Hazard

Using Geophysical Data and Probabilistic Approach," *J. Appl. Geophys.*, Vol. 68, No. 2, pp. 219–230.

Andrus, R. D., Piratheepan, P., Ellis, B. S., Zhang, J., and Juang, C. H., 2004, "Comparing Liquefaction Evaluation Methods Using Penetration-Vs Relationships," *Soil. Dyn. Earthquake Eng.*, Vol. 24, pp. 713–721.

Andrus, R. D. and Stokoe, K. H. II, 2000, "Liquefaction Resistance of Soils from Shear-Wave Velocity," *J. Geotech. Geoenviron. Eng.*, Vol. 126, No.11, pp. 1015–1025.

Cetin, K. O., Seed, R. B., Kiureghian, A. D., Tokimatsu, K., Harder, L. F., Jr., Kayen, R. E., and Moss, R. E. S., 2004, "Standard Penetration Test-Based Probabilistic and Deterministic Assessment of Seismic Soil Liquefaction Potential," *J. Geotech. Geoenviron. Eng.*, Vol. 130, pp. 1314–1340.

Indian Standard IS 2132, 1986, "Code of Practice for Thin-Walled Tube Sampling of Soils," Compendium of Indian Standards on Soil Engineering—Part 2, Bureau of Indian Standards, New Delhi, pp. 166–168.

Farrar, J. A., Nickell, J., Alien, M. G., Goble, G., and Berger, J., 1998, "Energy Loss in Long Rod Penetration Testing—Terminus Dam Liquefaction Investigation," *Proceedings of the ASCE Specialty Conference on Geotechnical Earthquake Engineering and Soil Dynamics III*, Seattle, Washington, Vol. 75, pp. 554–567.

GovindaRaju, L., Ramana, G. V., HanumanthaRao, C., and Sitharam, T. G., 2004, "Site Specific Ground Response Analysis," Special Section, Geotechnics and Earthquake Hazards*Curr. Sci.*, Vol. 87, No.10, pp. 1354–1362.

IBC, 2006, *International Building Code*, 1st ed., International Code Council, Inc., Falls Church, VA.

Idriss, I. M. and Boulanger, R. W., 2004, "Semi Empirical Procedures for Evaluating Liquefaction Potential During Earthquakes," *Proc. of the 11th International Conference on Soil Dynamics and Earthquake Engineering and the Third International Conference on Earthquake Geotechnical Engineering*, Berkeley, CA, D. Doolin et al., Eds., Stallion Press, Vol. 1, pp. 32–56.

Imai, T. and Tonouchi, K., 1982, "Correlation of N-Value with S-Wave Velocity and Shear Modulus," *Proceedings of the Second European Symposium on Penetration Testing*, Amsterdam, pp. 57–72.

Juang, C. H., Jiang, T., and Andrus, R. D., 2002, "Assessing Probability-Based Methods for Liquefaction Potential Evaluation," *J. Geotech. Geoenviron. Eng.*, Vol. 128(7), pp. 580–589.

Kanlı, A. I., Tildy, P., Pronay, Z., Pinar, A., and Hemann, L., 2006, "Vs30 Mapping and Soil Classification for Seismic Site Effect Evaluation in Dinar Region, SW Turkey," *Geophys. J. Int.*, Vol. 165, pp. 223–235.

Kayen, R. E., Mitchell, J. K., Seed, R. B., Lodge, A., Nishio, S., and Coutinho, R., 1992, "Evaluation of SPT-, CPT-, and Shear Wave-Based Methods for Liquefaction Potential Assessment Using Loma Prieta Data," *Proc. of the Fourth Japan-U.S. Workshop on Earthquake-Resistant Des. of Lifeline Fac. and Countermeasures for Soil Liquefaction*, NCEER-90-0019, I. M. Hamada and T. D. O'Rourke, Eds., Nat. ctr. for earthquake Engre. Res. (NCEER), State Univ. of New York at Buffalo, NY, Vol. 1, pp. 177–204.

Kovacs, W. D., Salomone, L. A., and Yokel, F. Y., 1981, *Energy Measurement in the Standard Penetration Test*, U.S. Department of Commerce and National Bureau of Standards, Washington, D.C.

Kramer, S. L., 1996, *Geotechnical Earthquake Engineering*, Pearson Education Ptd. Ltd., Delhi, India, reprinted 2003.

Liao, S. S. C. and Whitman, R. V., 1986, "Catalogue of Liquefaction and Non-Liquefaction Occurrences During Earthquakes," ,*Research Rep. Prepared for Dept. of Civil Eng.*, Massachusetts Institute of Technology, Cambridge, MA.

Miller, R. D., Xia, J., Park, C. B., and Ivanov, J., 1999, "Multichannel Analysis of Surface Waves to Map Bedrock," *The Leading Edge*, Vol. 18, No. 12, pp. 1392–1396.

Motulsky, H., 2008, Confidence and Prediction Bands, Graphing Nonlinear Regression, GraphPad Prism version 5.00 for Windows, GraphPad Software, San Diego, California, USA, http://www.graphpad.com (Last accessed 23 August 2008).

Ohta, Y. and Goto, N., 1978, "Estimation of S-Wave Velocity in Terms of Characteristic Indices of Soil," *Butsuri-Tanko(Geophysical Exploration)*, Vol. 29, No. 4, pp. 34–41 (in Japanese).

Park, C. B., Miller, R. D., and Miura, H., 2002, "Optimum Field Parameters of an MASW Survey," *Proceedings of the SEG-Japan 2002*, Japan, Tokyo, Vol. 1, pp. 22–23.

Park, C. B., Miller, R. D., and Xia, J., 1999, "Multi-Channel Analysis of Surface Waves," *Geophysics*, Vol. 64, No. 3, pp. 800–808.

Pearce, J. T. and Baldwin, J. N., 2005, "Liquefaction Susceptibility Mapping St. Louis, Missouri, and Illinois," *Final Technical Report*, published in web.er.usgs.gov/reports/abstract/2003/cu/03HQGR0029.pdf (Last accessed December 2008).

Robertson, P. K., Woeller, D. J., and Finn, W. D. L., 1992, "Seismic Cone Penetration Test for Evaluating Liquefaction Potential Under Cyclic Loading," *Can. Geotech. J.*, Vol. 29, pp. 686–695.

Robertson, P. K. and Wride, C. E., 1998, "Evaluating Cyclic Liquefaction Potential Using the Cone Penetration Test," *Can. Geotech. J.*, Vol. 35, No. 3, pp. 442–459.

Schmertmann, J. H. and Palacios, A., 1979, "Energy Dynamics of SPT," *J. Geotech. Engrg. Div.*, Vol. 105, No. GT8, pp. 909–926.

Seed, H. B. and Idriss, I. M., 1982, "Ground Motions and Soil Liquefaction during Earthquakes," *Monogr.* 5, Earthquake Engineering Research Institute, University of California, Berkeley.

Seed, H. B., Idriss, I. M., and Arango, I., 1983, "Evaluation of Liquefaction Potential Using Field Performance Data," *J. Geotech. Engrg.*, Vol. 109, No. 3, pp. 458–482.

Seed, H. B., Tokimatsu, K., Harder, L. F., and Chung, R. M., 1985, "The Influence of SPT Procedures in Soil Liquefaction Resistance Evaluations," *J. Geotech. Engrg.*, Vol. 111, No. 12, pp. 1425–1445.

Seed, H. B., Wong, R. T., Idriss, I. M., and Tokimatsu, K., 1986, "Moduli and Damping Factors for Dynamic Analyses of Cohesionless Soils," *J. Geotech. Engrg.* Vol. 112, No. 1, pp. 1016–1032.

Sitharam, T. G. and Anbazhagan, P., 2008a, "Seismic Microzonation: Principles, Practices and Experiments," EJGE Special Volume Bouquet 08, online, http://www.ejge.com/Bouquet08/Preface.htm (Last accessed December 2008), P-61.

Sitharam, T. G. and Anbazhagan, P., 2008b, "Evaluation of Low Strain Dynamic Properties Using Geophysical Method: A Case Study," *Consulting Ahead*, Vol. 2, No. 2, pp. 34–50.

Sitharam, T. G., Anbazhagan, P., and Mahesh, G. U., 2007, "3-D Subsurface Modelling and Preliminary Liquefaction Hazard Mapping of Bangalore City Using SPT Data and GIS," *Indian Geotechnical Journal*, Vol. 37, pp. 210–226.

Sitharam, T. G., Srinivasa Murthy, B. R., and Kolge, A., 2001, "A Post-Mortem of the Collapse of Structures in Ahmedabad During the Bhuj Earthquake, *Proceedings of the Indian Geotechnical Conference*, IGC-2001, Indore, IGS, Vol. 1, pp. 344–347.

Sivrikaya, O. and Toğrol, E., 2006, "Determination of Undrained Strength of Fine-Grained Soils by Means of SPT and Its Application in Turkey," *Eng. Geol.*, Vol. 86, pp. 52–69.

Skempton, A. W., 1986, "Standard Penetration Test Procedures," *Geotechnique*, Vol. 36, No. 3, pp. 425–447.

Sykora, D. W., 1987, "Creation of a Data Base of Seismic Shear Wave Velocities for Correlation Analysis," *Geotech. Lab. Miscellaneous Paper* GL-87-26, U.S. Army Engineer Waterways Experiment Station, Vicksburg, MS.

Xia, J., Miller, R. D., and Park, C. B., 1999, "Estimation of Near-Surface Shear-Wave Velocity by Inversion of Rayleigh Wave," *Geophysics*, Vol. 64, No. 3, pp. 691–700.

Yilmaz, I. and Bagci, A., 2006, "Soil Liquefaction Susceptibility and Hazard Mapping in the Residential Area of Kutahya (Turkey)," *Environ. Geol.*, Vol. 49, pp. 708–719.

Youd, T. L., Idriss, I. M., Andrus, R. D., Arango, I., Castro, G., Christian, J. T., Dobry, R., Liam Finn, W. D., Harder, L. H. Jr., Hynes, M. E., Ishihara, K., Koester, J. P., Liao, S. S. C., Marcuson, W. F., Marting, G. R., Mitchell, J. K., Moriwaki, Y., Power, M. S., Robertson, P. K., Seed, R. B., and And Stokoe, K. H., 2001, "Liquefaction Resistance of Soils: Summary from the 1996 NCEER and 1998 NCEER/NSF Workshops on Evaluation of Liquefaction Resistance of Soils," *J. Geotech. Geoenviron. Eng.*, Vol. 127, No. 10, pp. 817–833.